

# High speed inductive position sensor for E-machines

L. Lugani<sup>1</sup>, Y. Akermi<sup>1</sup>, P. Laval<sup>2</sup>, A. Duisters<sup>1</sup>

1: Melexis Technologies SA, Chemin de Buchaux 38, 2022 Bevaix, Switzerland

2: Melexis NV/BO France, ZI Les Bois de Grasse, 7 Av. M. Chevalier, Le Cube Business, 06130 Grasse, France

**Abstract:** This paper presents a new inductive resolver solution, based on a newly developed interface integrated circuit with Sine/Cosine output: the MLX90510. This sensor interface is based on a 3-phase coil approach and uses smart digital signal processing to reach a high accuracy of  $\pm 0.36^\circ$  el. up to 240'000 e-rpm and, and achieve ASIL-C automotive safety integrity level. The solution offers also a linearization feature to compensate for extra errors coming from mechanical tolerances.

**Keywords:** Inductive sensing, resolver, stray field immunity, ASIL C, high speed digital interface

## 1. Introduction

Electric and hybrid vehicles' E-traction motors (E-machines) are key safety critical components in the powertrain of the future. The main challenge relies on the synchronization of the stator supply currents with the rotor position, leading to an optimal efficiency and torque characteristic control. An error in the rotor position is leading to an error in the synchronization of the stator currents which will immediately lower the overall performance of the system, if not leading to a safety issue. Therefore, the key requirements for a rotor position sensor are:

- Reliable and accurate ( $<1^\circ$  el.) position sensing up to 240'000 e-rpm
- Immunity against magnetic stray-fields
- High automotive safety integrity level up to ASIL D
- Scalability for different motor designs and sensor placements
- Light weight and cost efficiency

Today the most commonly used position sensor in traction motors is the Variable Reluctance resolver (VR resolver) consisting of a ferromagnetic rotor and a stator with several secondary coils [1]. VR resolvers, although having a long track record in E-machine position sensing applications, present some disadvantages, in particular their high cost and high weight.

An excellent alternative to cover these requirements are the inductive position sensors.

On one hand they combine a high accuracy over a wide speed range, immunity against stray fields and enable ASIL-D automotive safety integrity level. On the other hand, they reduce the overall cost of an electric drivetrain compared to VR resolver technology.

Figure 1 illustrates how the inductive resolver integrates in the E-machine.

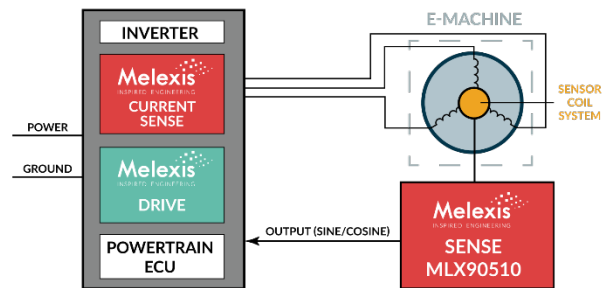


Figure 1: Motor control System overview with an analog Sine/Cosine communication protocol

In inductive position sensors the transducer is a coil set composed of a transmission (Tx) coil and receiving (Rx) coils, connected to an inductive position sensor interface integrated circuit (IC). The design is complemented with a metallic target attached to the E-machine (Rotor) which needs to be sensed. The position sensor interface IC converts the input signals from the Rx coils into differential Sine/Cosine output signals. The signals are used to communicate with the ECU. The only computation the ECU has to perform is an angle calculation out of the Sine/Cosine signals by an arc tangent operation.

In this paper we present a new inductive resolver solution, based on a newly developed interface IC: with Sine/Cosine output: the MLX90510. This sensor interface uses smart digital signal processing to reach a high accuracy of  $\pm 0.36^\circ$  el. over its wide operating conditions, and achieve ASIL-C automotive safety integrity level. The sensor works with a 3-phase coil set, which brings further advantages discussed in the document.

The paper is organized as follows. Section 2 describes the basic principles of inductive sensing. Section 3 details how the inductive coil set is designed and how it adapts to the number of pole pairs of the E-machine. The MLX90510 IC is then presented in section 4. We explain in section 5 the reasons behind the chosen 3-phase coils approach versus a more classical quadrature one. Section 6 focuses on the various sensing modes. Section 7 explains how the linearization feature of the MLX90510 can mitigate errors. Finally, section 8 provides an outlook to a future High Speed (HS) digital communication protocol. This aims at further optimizations of the system cost while increasing its reliability.

## 2. Basic principles of inductive sensors

Inductive position sensors measure the position of a metallic target which is placed in front of a set of inductive coils [2]. As this paper is focused on E-machine applications, we consider only angular sensors. A typical sensor configuration is depicted in Figure 2. In these applications a metallic target is attached to the motor rotor. It consists of a number of lobes matching the number of pole pairs of the motor. The coils are on the other hand fixed to the motor stator and are generally manufactured in PCB technology. The coils are in turn connected to the integrated circuit interface. The MLX90510 chip, whose function is to drive and read voltages from the coils, computes the “target” angle from the received signals and outputs the calculated value in the form of a differential SIN/COS.

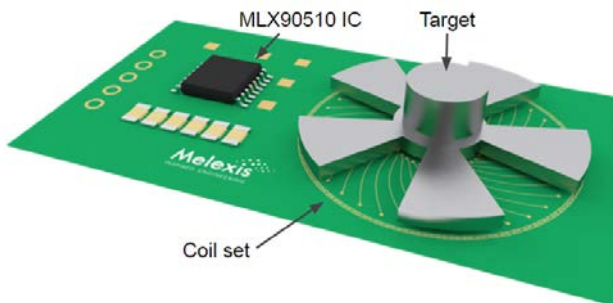


Figure 2: Example of an inductive sensor board

The basic working principle of the sensor is illustrated in Figure 3. Within the coil set, we can distinguish a circular coil, the transmission (Tx) coil, whose role is to generate a cylindrically symmetric AC magnetic field. For this reason, the Tx coil is actively driven by the interface IC at the carrier frequency, which for our solution lies in the 2-5 MHz range. To minimize current consumption, the Tx coil is put in resonance by means of resonance capacitors. The Tx coil field excites eddy currents in the target, which generates a secondary field, named the target field. As the target consists of a number of lobes, the target field does not have cylindrical symmetry, but has an angular dependency. The target field period in the angular domain corresponds to the angular sector encompassed by two adjacent target lobes, i.e.  $360^\circ/N$ , where  $N$  is the number of pole pairs of the motor. This angular span is also referred to as an electrical period and is defined to be equal to  $360^\circ$  electrical ( $1^\circ$  el. =  $1^\circ/N$  mech.).

The receiving (Rx) coils are designed to capture the target field while being insensitive to the Tx field. This is accomplished by winding each Rx coil in such a way that every electrical period contains two loops connected in series, the first turning in the clockwise direction and the second in the counter clockwise direction. The cylindrically symmetric Tx field is thus rejected as it induces opposite voltages in the two loops, while the target field is captured due to the matching periodicity. As the target rotates, the

Rx coil generates an AC voltage at the carrier frequency characterized by an amplitude modulation envelope which is approximately sinusoidal over an electrical period (see Figure 5d). By optimizing the Rx coil shape, the envelope profile can be made closer to an ideal sinusoid.

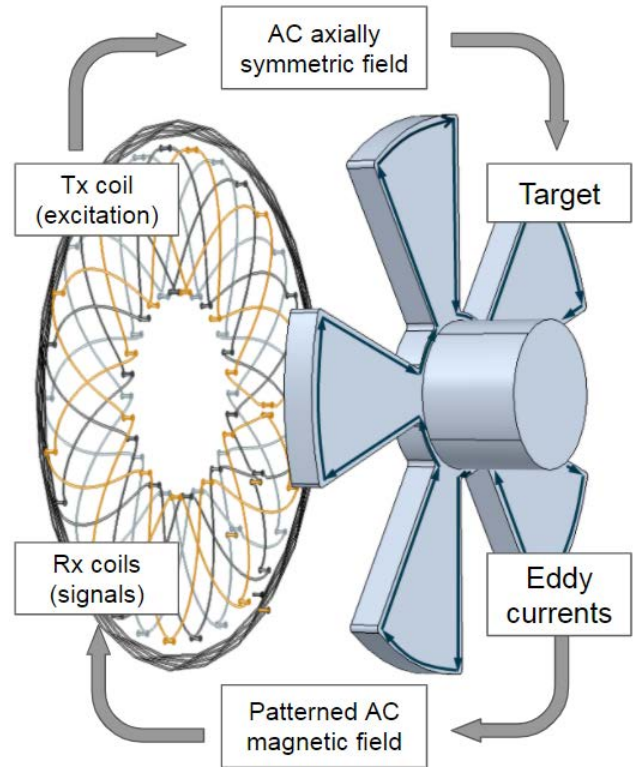


Figure 3: Inductive sensing principle

The sensor makes use of the multiple Rx coils in order to allow a ratiometric angle calculation independent from the signal strength. In the solution we propose we make use of a 3-phase Rx coil set, where the individual Rx coils are displaced by  $120^\circ$  el. one with respect to each other. The reasons behind this choice versus an apparently simpler pair of Rx coils in quadrature configuration is discussed in the Section 5.

## 3. Coil design and design scalability

The fact that in inductive sensors the transducer, i.e. the coil set, is implemented in the PCB design and not integrated in the interface chip provides a great degree of flexibility in their design. Most importantly, the periodicity of the coil arrangement can be tailored at will and in particular adapted to the number of pole pairs of the device.

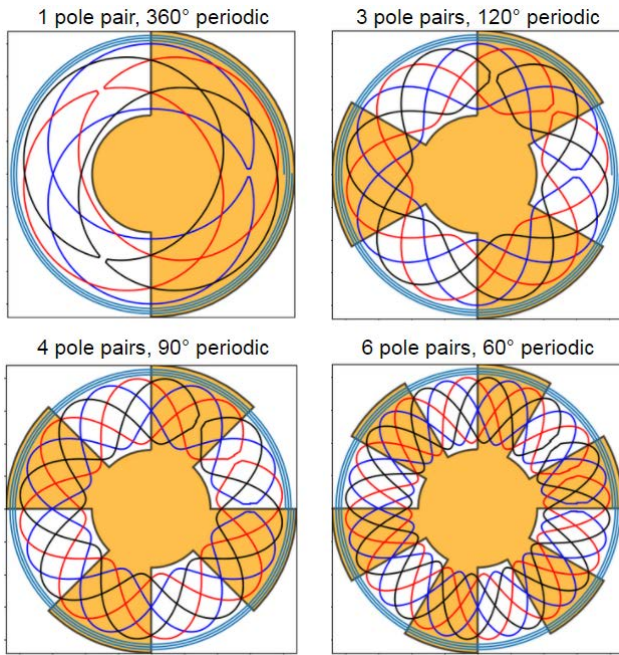


Figure 4: Examples of inductive sensor with different periodicity

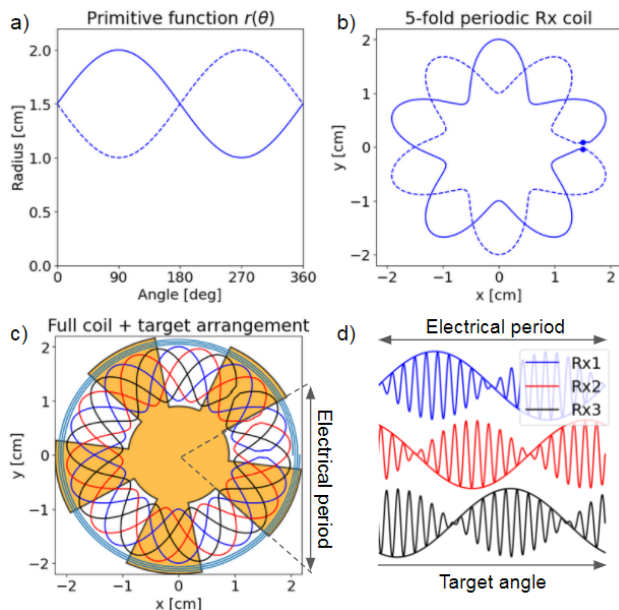


Figure 5: Coil design flow of a 5 pole pairs, 4 cm diameter inductive sensor. a) primitive function. b) individual Rx coil pattern. c) Full coil set plus target d) Rx voltages over an electrical period.

Figure 4 shows some examples of coil design with variable periodicity. This allows matching the sensor range with the motor electrical period, thus maximizing the sensor accuracy. There is no theoretical maximum number of pole pairs an inductive sensor can accommodate, but a limitation mainly coming from space and PCB design rule constraints.

Figure 5 illustrates schematically how the coil set is obtained. The Rx coils are defined from a sinusoidal primitive function  $r(\theta) = R_0 + \Delta R \sin(\theta)$  and its complementary one  $r'(\theta) = R_0 - \Delta R \sin(\theta)$  (Figure 5a). The Rx coil pattern is then obtained by means of a polar coordinate transformation, with the attention to fit N periods in a full turn, N being the number of pole pairs of the motor (Figure 5b):

$$\begin{cases} x = r(N\theta) \cos(\theta) \\ y = r(N\theta) \sin(\theta) \end{cases} \quad [1]$$

The full coil set is then completed by adding two other Rx coils, shifted by  $120^\circ/N$ , a circular Tx coil around the Rx coils and a target (Figure 5c). This configuration will provide a 3-phase signal set as sketched in Figure 5d).

#### 4. MLX90510 IC architecture

The block diagram of the MLX90510 inductive sensor interface IC is detailed in Figure 6. The device is a mixed signal IC which include an analog and a digital domain. The analog part of the IC takes care of driving the Tx coil via an LC oscillator, and treating the Rx signals, which are filtered, amplified and rectified before being digitalized. The digitalized signals are then fed to the digital signal processing chain, which implements a tracking loop computing the phase, speed and acceleration of the rotor. This information is used in order to compute a delay compensated angle. The differential SIN/COS output is finally synthesized by means of two digital to analog converters and fed to the output drivers.

This architecture based on a DSP differs significantly with respect to other analog based implementations used in combination with quadrature coils. The digital based approach allows to implement a number of advantageous features.

First, the fact that the output signals are synthesized from a digital angle implies that they have well defined and stable amplitudes, independent of the Rx signals strength. Considering that the received signals amplitude is strongly airgap dependent, this implies that airgap variations will not affect the output signal strength.

A second important advantage of the digital architecture is that it allows achieving an extremely low propagation delay. Propagation delay, i.e. the time taken by the signals to undergo the IC signal chain, directly impacts the angular error, giving a contribution proportional to the rotor speed. Analog based solutions can't avoid propagation delay related errors, which are in the range of  $\sim 3 \mu s$  [3] and are furthermore temperature dependent. For a rotor speed of 100'000 e-rpm, this implies errors already exceeding  $3^\circ$  el. In our solution the propagation delay is trimmed over temperature during the final test of the

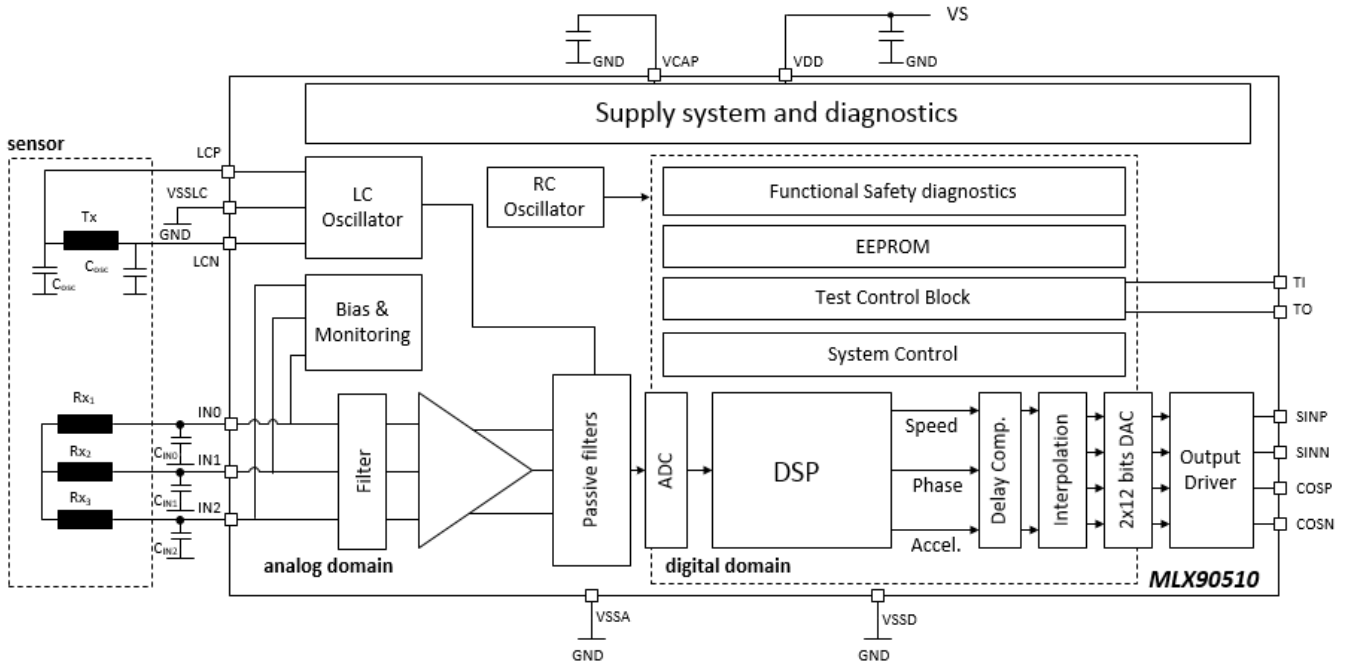


Figure 6: Block diagram of the MLX90510 IC

device, allowing the digital processing chain to compensate for it. We therefore achieve, on average, 0 propagation delay, with low residual variation of  $\pm 100$  ns due to finite trimming accuracy. Thanks to this important feature, we are able to guarantee an accuracy of the MLX90510 interface of  $\pm 0.36^\circ$  el. over the full  $-40^\circ\text{C}$  to  $160^\circ\text{C}$  operating temperature range and up to speeds of 240'000 rpm el.

Finally, the chosen architecture allows for the implementation of a number of safety monitors. This will assure that the delivered Sine/Cosine output signals are ASIL C fail-safe compliant without the need for external safety measures from the ECU. The communication of a detected failure is accomplished by switching the output pins to high-Z state.

### 5. Advantages of the 3-phase sensor concept

The choice made in our solution to use a 3-phase coil set rather than a more classical SIN/COS pair deserves some discussion. In this section we will show how this approach allows reaching a better linearity by filtering some unwanted harmonics in the Rx signals.

In an ideal case, we would want that the Rx signals envelope evolves with the target angle according to a perfect sinusoid. However, this is not the case. The Rx signals will contain unwanted harmonics, simply because the target field is not a purely sinusoidal field pattern.

The target magnetic field  $\vec{B}e^{i\omega t}$  can be written, in cylindrical coordinates, as an harmonic series:

$$\vec{B}(r, \theta, z) = \sum_{i=0}^{\infty} \vec{B}_i(r, z) \cos(Ni\theta - i\alpha) \quad [2]$$

Due to exposure to the target field, the three Rx coils will as a consequence generate the signals  $v_i e^{i\omega t}$ ,  $i=1, 2, 3$ :

$$\begin{cases} v_1 = \sum_{i=0}^{\infty} w_i \cos(i\alpha) \\ v_2 = \sum_{i=0}^{\infty} w_i \cos\left(i\alpha - i\frac{2\pi}{3}\right) \\ v_3 = \sum_{i=0}^{\infty} w_i \cos\left(i\alpha + i\frac{2\pi}{3}\right) \end{cases} \quad [3]$$

The various harmonic coefficients  $w_i$  of the Rx signals are given as the surface integral of the target field on one of the Rx coil, we take coil 1 as reference:

$$w_i = \int_{S_1} [\vec{B}_i(r, z) \cdot \hat{n}] \cos(Ni\theta) dS \quad [4]$$

Where  $S_1$  is the surface of Rx coil 1 and  $\hat{n}$  its normal vector.  $w_1$  is the useful signal, while all the other harmonics are unwanted and can be source of angular error. All the even harmonics are rejected by the coil system due to the presence of the two clockwise and counter clockwise turning loops per electrical period. Odd harmonics are on the other hand not rejected and enter the signal chain. Given that the intensity of the various harmonics decreases with increasing order, we would expect that the intrinsic error of an inductive sensor (i.e. the error of a perfectly aligned system where feeding wires do not introduce additional errors) is dominated by the effect of the 3<sup>rd</sup> harmonic component of the signals. This is indeed the case for a quadrature system, where a simple calculation shows that the intrinsic error is given by:

$$\varepsilon_{quadrature} = -\frac{w_3}{w_1} \sin(4\alpha) \quad [5]$$



In our 3-phase solution, however, the signals undergo differential amplification, which results in a new signal set  $s_i$ :

$$\begin{cases} s_1 = \sum_{i=0}^{\infty} w_i \left[ \cos(i\alpha) - \cos\left(i\alpha - i\frac{2\pi}{3}\right) \right] \\ s_2 = \sum_{i=0}^{\infty} w_i \left[ \cos\left(i\alpha - i\frac{2\pi}{3}\right) - \cos\left(i\alpha + i\frac{2\pi}{3}\right) \right] \\ s_3 = \sum_{i=0}^{\infty} w_i \left[ \cos\left(i\alpha + i\frac{2\pi}{3}\right) - \cos(i\alpha) \right] \end{cases} \quad [6]$$

It can be easily seen that in this new signal set the 3<sup>rd</sup> harmonic is suppressed as the angular factors cancel out for  $i=3$ . In our 3-phase approach the intrinsic error is thus dominated by 5<sup>th</sup> and 7<sup>th</sup> harmonic components, which can be shown to generate the following error:

$$\epsilon_{triphase} = -\frac{w_7 - w_5}{w_1} \sin(6\alpha) \quad [7]$$

Given that 5<sup>th</sup> and 7<sup>th</sup> harmonics are much weaker than 3<sup>rd</sup> harmonic components, our 3-phase approach provides a better linearity with respect to a classical quadrature approach. This is well illustrated in Figure 7 where the intrinsic errors of a quadrature and 3-phase 360° sensor are compared. We see a dominant 4<sup>th</sup> harmonic error component in the quadrature design, consistently with previous reports [4], which is absent in the 3-phase design.

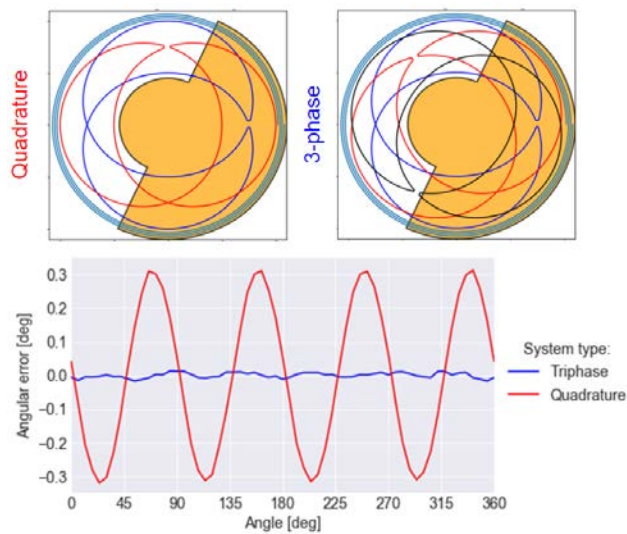


Figure 7: Comparison of the intrinsic error of a quadrature and 3-phase 360° inductive sensor. The quadrature system provides a relatively strong 4<sup>th</sup> harmonic error component, while the 3-phase system only provides a weak 6<sup>th</sup> harmonic component

## 6. Sensing modes

The coil design flexibility enabled by PCB technology allows also adapting the inductive sensor layout to different sensing modes. Figure 8 illustrates the 3 main sensing modes possible, i.e. end of shaft, through shaft and side of shaft.

In through shaft and side of shaft modes the coils span the whole 360° circle. We name such coil designs “O-shaped” The main difference between the two modes is that in the

end of shaft configuration the coils can be made quite small, while in through shaft mode the fact that the shaft passes in the middle of the PCB implies that the coil dimensions are relatively large. In some cases, this may result in relatively high PCB cost. The side of shaft approach becomes in this case interesting, at least from a cost perspective. In these designs, the Rx coils do not span all the electrical periods, but only one or few of them. The Tx coil runs around the Rx coils, forming a circular arc shape. We thus name these designs “C-shaped”.

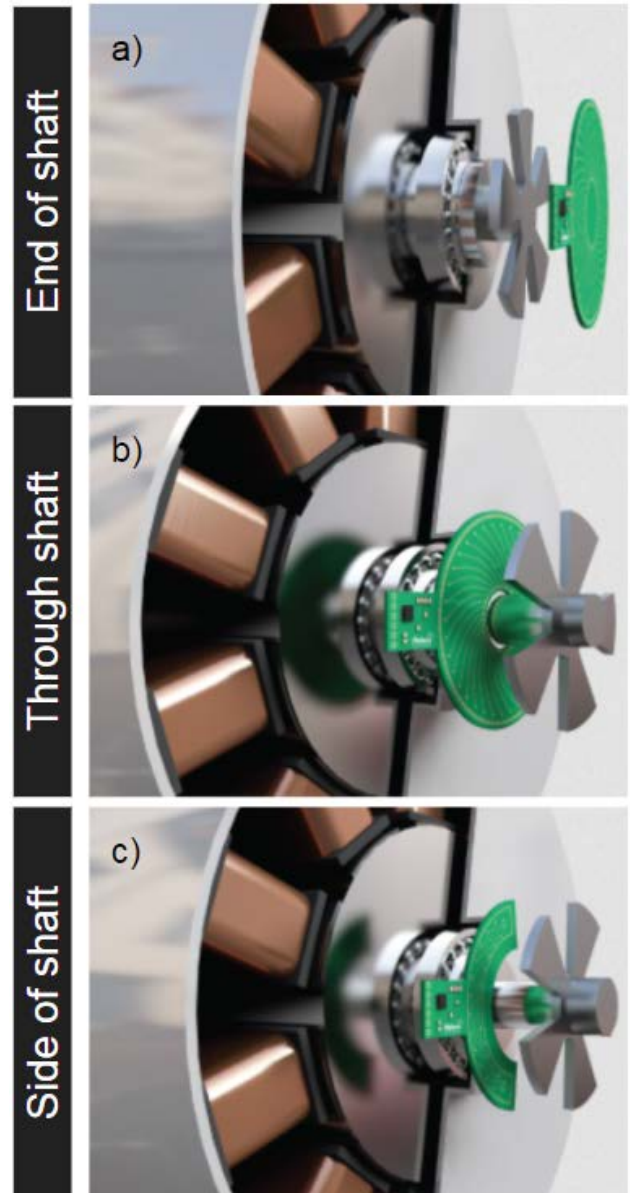


Figure 8: Inductive sensing modes: a) end of shaft, b) through shaft, c) side of shaft

The various sensing modes do not differ only for the cost aspect. They are also different with respect to the accuracy dimension. An O-shaped sensor is more accurate than a C-shaped sensor, and the ultimate reason for this difference comes from the fact that in O-shaped designs

we have multiple Rx coil periods spanning the whole circle, while in C-shaped sensors there are only one or some Rx coil periods available. This affects both the intrinsic accuracy of the sensor, i.e. the accuracy under perfect alignment, as well as the sensitivity to mechanical tolerances.

The intrinsic accuracy of an O-shaped design is very good. Indeed, for whatever angular position the target overlaps completely with the Tx coil. As a consequence, the eddy current pattern in the target is independent from the angle. In C-shaped sensors, on the other hand, the overlap between the target and the Tx coil depends on the angle, as inevitably a given tooth will enter or exit the Tx coil area for some angles. This translates in an angle dependent eddy current pattern in the target, resulting in angular errors. In addition, C-shaped sensors are quite sensitive to mechanical tolerances, while O-shaped sensors are quite robust with respect to misalignments. In the case of an O-shaped design, shown a misalignment will generate different errors in the various electrical periods, with the total error averaging to zero. This averaging effect is clearly not present or only partially achievable in a C-shaped design.

Figure 9 illustrates with a practical example this difference. The graph compares the error curves of two 5 pole pairs designs under good alignment. The C-shaped sensor shows clearly higher errors, coming both from a higher intrinsic error but also from slight misalignments in the measurement setup.

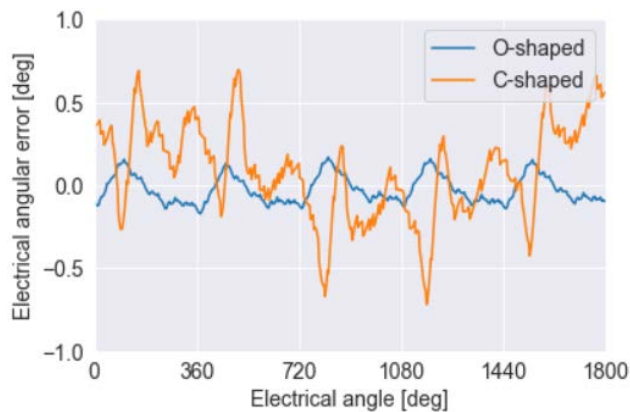


Figure 9: Example of error curves for 5 pole pairs O- and C-shaped designs over a full rotation. Note the higher error of the C-shaped design

### 7. Linearization

The error budget of an inductive sensor can be decomposed, on the basis of the discussions of the previous paragraphs, into the following components:

- Intrinsic error of the coils system (residual harmonics in the Rx signals, parasitic contributions from the coils feeding wires and from the surrounding metal environment)

- IC contributions
- Mechanical tolerances

None of these errors can be completely reduced to zero. In order to reach higher accuracy levels, the MLX90510 offers the possibility to program a 16 points piecewise linearization curve for error compensation. The method is particularly efficient and can deal even with complex error curve, however, it can act only on errors which repeat identically over the different electrical periods. While this is the case for most error contributors, some mechanical tolerances generate errors which are periodic only over one full 360° mechanical rotation. In addition to airgap deviations from the nominal value, there are four main mechanical tolerances that can be source of complex angular errors: off-axis, tilt, wobble and skew. They are sketched in Figure 10. Off-axis and tilt are providing errors which are periodic over a single electrical period. On the other hand, wobble and skew generate errors with full 360° mechanical turn periodicity, so errors which are not identical in the various electrical periods. These errors cannot be compensated by the linearization. However, wobble and skew are normally much less important than off-axis and tilt.

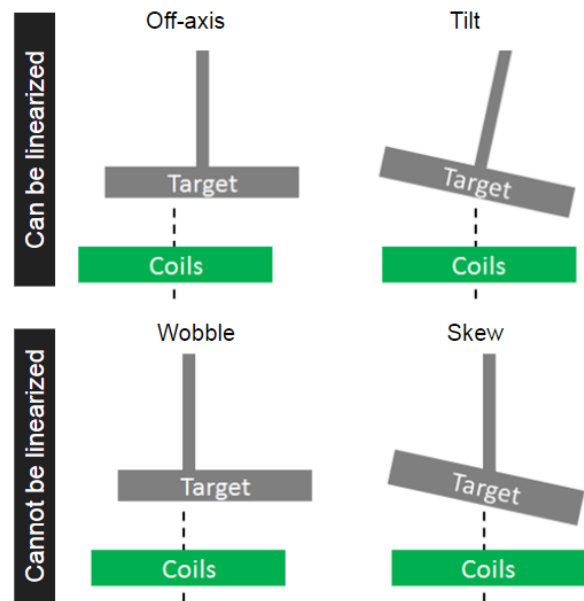


Figure 10: Mechanical tolerances type. Off-axis and tilt generate errors that can be linearized, while this is not the case for wobble and skew

Figure 11 illustrates how the linearization approach allows reaching high accuracy. The picture shows the measured error curve for a 4 pole pair design over a full 360° mechanical rotation, i.e. 4 electrical periods (1440° el.). We can distinguish that the  $\pm 0.5^\circ$  el. error can be decomposed into a component having the period of 360° el. and another having a period of 1440° el. Programming the MLX90510 with a linearization curve deduced from

the 360° el. periodic component results in a low residual error of  $\pm 0.25^\circ$  el.

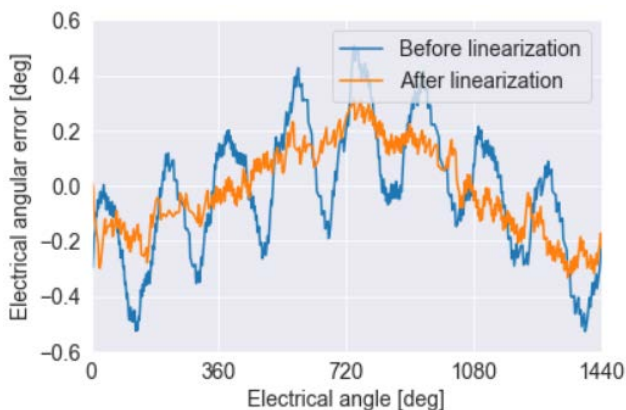


Figure 11: Error profile over a full mechanical turn for a 4 pole pair design before and after linearization.

## 9. Conclusions

In conclusion, the inductive position sensor technology offers many advantages. Its flexibility and scalability makes it the most suited solution for E-machine rotor position sensing.

## 10. References

- [1] X. Ge, Z. Q. Zhu, R. Ren and J. T. Chen, "Analysis of Windings in Variable Reluctance Resolver," in *IEEE Transactions on Magnetics*, vol. 51, no. 5, pp. 1-10, May 2015, Art no. 8104810
- [2] Hobein, D., Dorißen, T., and Dürkopp, K., "Progress in Automotive Position Sensors and Introduction of the Hella Inductive Position Sensor," SAE Technical Paper 2004-01-1115, 2004
- [3] AS5715A/AS5715R On-/Off-Axis Inductive Position Sensor with Sin/Cos Output, AMS, 2020. Available: [https://ams.com/documents/20143/4390346/AS5715A-AS5715R\\_DS000511\\_3-00.pdf](https://ams.com/documents/20143/4390346/AS5715A-AS5715R_DS000511_3-00.pdf)
- [4] M. Passarotto, G. Qama and R. Specogna, "A Fast and Efficient Simulation Method for Inductive Position Sensors Design," 2019 IEEE SENSORS, 2019, pp. 1-4

*Devices sold by Melexis are covered by the warranty and patent indemnification provisions appearing in its Term of Sale. Melexis makes no warranty, express, statutory, implied, or by description regarding the information set forth herein or regarding the freedom of the devices and their use or combination in applications from patent infringement. The information furnished by Melexis is believed to be correct and accurate. However, Melexis shall not be liable to recipient or any third party for any damages, including but not limited to personal injury, property damage, loss of profits, loss of use, interrupt of business or indirect, special incidental or consequential damages, of any kind, in connection with or arising out of the furnishing, performance or use of the technical data herein. No obligation or liability to recipient or any third party shall arise or flow out of Melexis' rendering of technical or other services. Melexis reserves any of its or third party's intellectual property rights in relation to this document. This disclaimer and document will be governed and construed by Belgian law and any disputes relating to this disclaimer will be subject to the exclusive jurisdiction of the courts of Brussels, Belgium.*